

To appear in ApJ Letters Vol. 570, 10 May 2002.

## Detecting gravitational lensing cosmic shear from samples of several galaxies using two-dimensional spectral imaging

A. W. Blain

*Astronomy Department, Caltech 105-24, Pasadena, CA 91125*

`awb@astro.caltech.edu`

### ABSTRACT

Studies of weak gravitational lensing by large-scale structures require the measurement of the distortions introduced to the shapes of distant galaxies at the few percent level by anisotropic light deflection along the line of sight. In order to detect this signal on 1'-10' scales in a particular field, accurate measurements of correlations between the shapes of order  $10^3$ - $10^4$  galaxies are required. This large-scale averaging is required to accommodate the unknown intrinsic shapes of the background galaxies, even with careful removal of systematic effects. Here an alternative is discussed. If it is possible to measure accurately the detailed dynamical structure of the background galaxies, in particular rotating disks, then it should be possible to measure directly the cosmic shear distortion since it generally leads to a non-self-consistent rotation curve. Narrow spectral lines and an excellent two-dimensional spatial resolution are required. The ideal lines are CO rotational transitions, and the ideal telescope is the Atacama Large Millimeter Array (ALMA).

*Subject headings:* galaxies: ISM — galaxies: kinematics and dynamics — galaxies: spiral — gravitational lensing — radio lines: galaxies

### 1. Introduction

Weak gravitational lensing is a valuable tool for studying the mass distribution along and around the line of sight to distant galaxies (Bartelmann & Schneider 2001). Away from galaxies and clusters, the effect is small: the axis ratio of high-redshift galaxies is modified by a few percent. Because the intrinsic shapes of distant galaxies are not known, it is necessary

to stack many thousands of galaxy images to detect a signal. This requires large, high-quality images, and so cosmic shear can only be detected statistically over areas extending more than about  $0''.5$ . Cosmic shear has been detected in both deep optical images (Bacon, Refregier & Ellis 2000; Wittman et al. 2000; Maoli et al. 2001; Pirzkal et al. 2001; van Waerbeke et al. 2001; Wilson, Kaiser & Luppino 2001) and very wide, shallow optical surveys (Fischer et al. 2000), but at present it is not possible to measure the shear towards a specific point on the sky.

Here we investigate the possibility of detecting weak lensing in observations of *individual* galaxies, by obtaining high-fidelity, two-dimensional, resolved spectroscopic measurements of morphology and dynamics. This may be possible using an integral field unit (IFU) adaptive optics (AO) optical or near-infrared(IR) spectrograph to image the narrow stellar absorption and hydrogen recombination lines. It should definitely be possible using the interferometric imaging of CO rotation line emission at millimeter wavelengths using the Atacama Large Millimeter Array (ALMA; Wootten 2001), or using meter-wave HI imaging using a Square Kilometer Array (SKA)<sup>1</sup> radio interferometer.

Measuring cosmic shear galaxy by galaxy would provide many new scientific opportunities, and a very valuable check on systematic errors in conventional techniques. Along several closely spaced lines of sight, a tomographic survey of the mass distribution out into the distant Universe could be made. The properties of the weak lensing shear field on very small (arcsec) galactic scales are unknown. Substructure in dark matter halos could lead to significant variations in the shear field on these scales. This would be washed out by averaging over both arcminute-scale fields in existing cosmic shear surveys (Pirzkal et al. 2001) and the stacked images analyzed for galaxy-galaxy lensing around the positions of bright galaxies (McKay et al. 2002).

## 2. The effect of weak lensing shear on rotation curves

We consider the illustrative case of representing a galaxy as an inclined rotating circular ring centered on the origin, with an inclination angle  $i$  between the rotation axis and the line of sight. The position angle (P.A.) of the projected elliptical ring on the sky is free to vary. The line-of-sight velocity of a point on the ring  $v \propto \sin i \cos \Phi$ , where  $\Phi$  is the angle between the point and the major axis of the ellipse. The dependence of the radial position and the line-of-sight velocity of a point on the ring on  $\Phi$  are shown for a model with  $i = 0.57$  rad ( $\simeq 33^\circ$ ) in Figures 1 and 2.

---

<sup>1</sup>[www.ras.ucalgary.ca/SKA/ska\\_science.shtml](http://www.ras.ucalgary.ca/SKA/ska_science.shtml)

Weak gravitational lensing shears the ellipse without changing its area (Schneider, Ehlers & Falco 1992). The transformation of angular position  $(\theta_x, \theta_y)$  to  $(\theta'_x, \theta'_y)$  due to lensing by a shear field  $\vec{\gamma} = (\gamma_1, \gamma_2)$  is described by

$$\begin{pmatrix} \theta'_x \\ \theta'_y \end{pmatrix} = \begin{pmatrix} 1 - \kappa - \gamma_1 & -\gamma_2 \\ -\gamma_2 & 1 - \kappa + \gamma_1 \end{pmatrix} \begin{pmatrix} \theta_x \\ \theta_y \end{pmatrix}. \quad (1)$$

In the weak lensing regime,  $\vec{\gamma}$  is small and the convergence  $\kappa \simeq 1 - \sqrt{1 + |\gamma|^2} \simeq 0$ , with  $|\gamma|^2 = \gamma_1^2 + \gamma_2^2$ . The  $\gamma_2 = 0$  shear component is aligned along  $\theta_x = 0$ , while the  $\gamma_1 = 0$  component is aligned along  $\theta_x = \theta_y$ . The frequency of radiation is not affected by lensing, and so the line-of-sight velocity remains the same. The velocity and position of a ring is thus modified by weak lensing in a straightforward way.<sup>2</sup>

Weak lensing by a large 10% shear field ( $|\gamma| = 0.1$ ) aligned in different directions is illustrated in Figures 1 and 2 for a galaxy with P.A. = 0 and  $i = 0.57$  rad. In most orientations, the effect of lensing is similar to modifying the P.A. and  $i$ . If  $\vec{\gamma}$  is perpendicular to the projected rotation axis, as shown in the second to leftmost panel of Figure 1, then the effect of shear is indistinguishable from modifying  $i$ . Based on position data alone, there is always a degeneracy between  $\vec{\gamma}$ ,  $i$  and P.A. However, velocity data reduces the degeneracy significantly. As shown by the bottom panel of Figure 2, the velocity field defines P.A. accurately, even when  $\vec{\gamma}$  is large.<sup>3</sup> Shear affects the position much more significantly than the velocity. If  $\vec{\gamma}$  is not perpendicular to the rotation axis, then the sheared ellipse cannot be

<sup>2</sup>The velocity field of strongly lensed giant arcs in clusters, for which  $\kappa$  is large, was discussed by Narasimha & Chitre (1993).

<sup>3</sup>This of course requires that the measured velocity field traces the general potential of the galaxy and is not affected strongly by a bar, a warp or a ‘lopsided’  $m_1$  asymmetry.

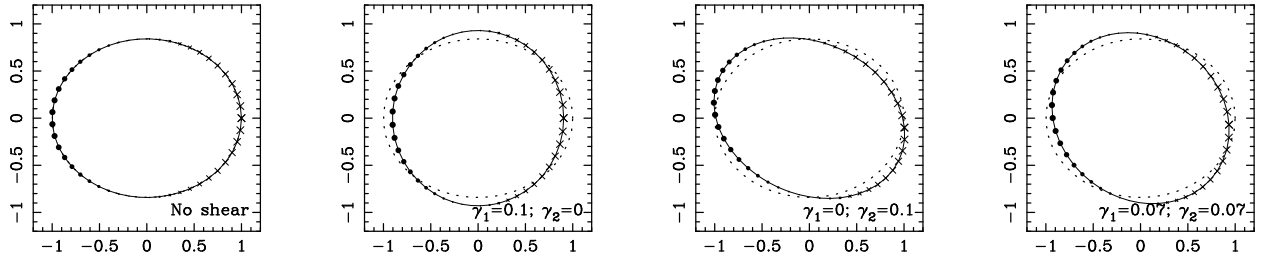


Fig. 1.— Position and line-of-sight velocity of points (*filled circles*, approaching; *crosses*, receding) on a rotating ring with  $i = 0.57$  rad/ $0^\circ.33$  and P.A. = 0 rad, with no weak lensing (*leftmost panel*) and for three large values of weak-lensing shear  $|\vec{\gamma}| = 0.1$  (*three rightmost panels*). The unlensed ring is shown by the dotted line for comparison.

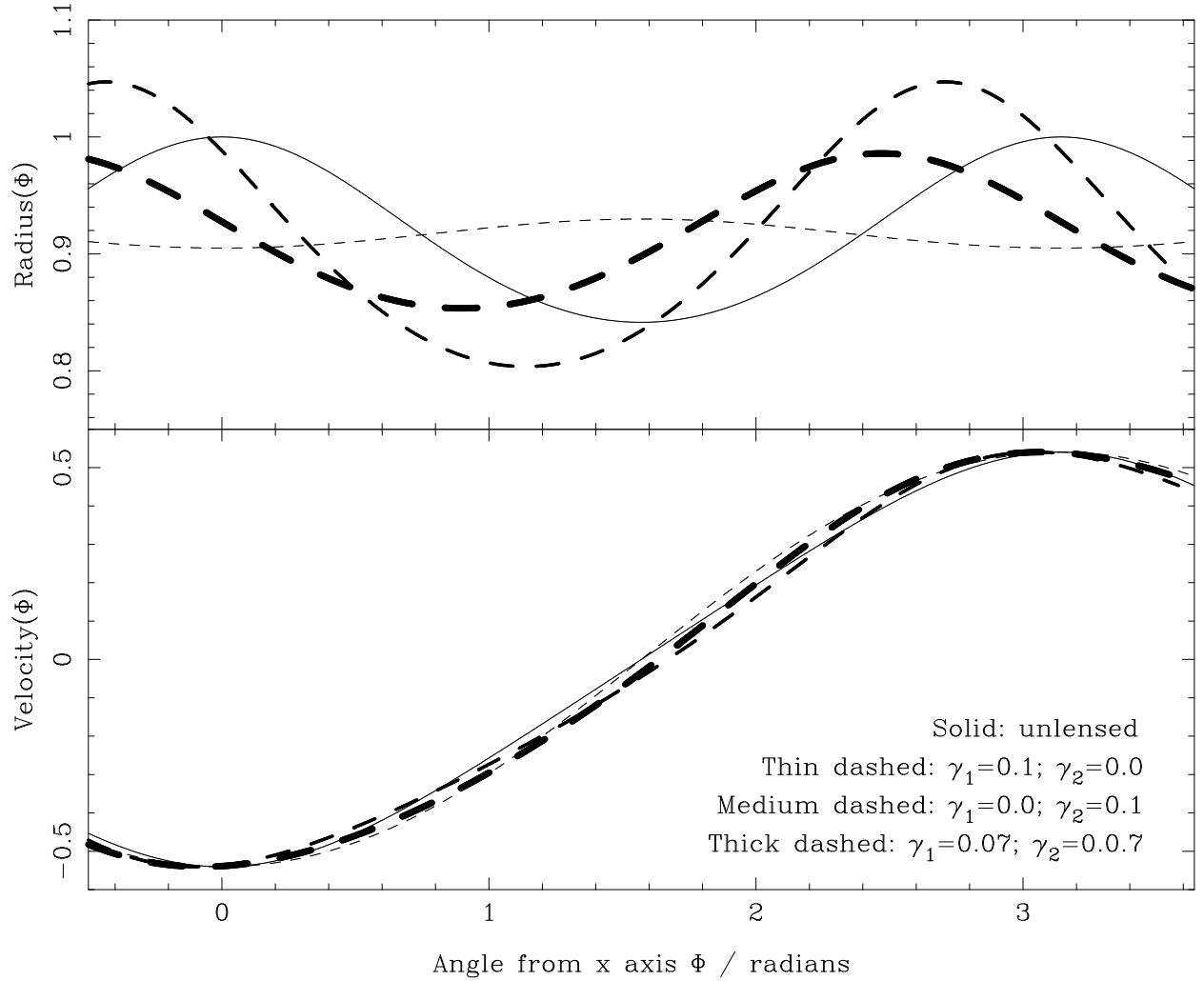


Fig. 2.— Radial distance and line-of-sight velocity of points on the ring shown in Fig. 1 as a function of angle on the sky  $\Phi$  over more than half of a circle. The solid and dashed lines show the results with zero and nonzero shear, respectively. Lensing has a more significant effect on radial position than velocity.

described self-consistently by a rotating ring: for example, neither shifting the radial curves in Figure 2 to the left or right, as expected for changing P.A., nor modifying the amplitude of their modulation, as expected for changing  $i$ , can fully mimic the effects of lensing if  $\gamma_2 \neq 0$ .

If sufficiently accurate spatially resolved two-dimensional spectroscopic images of a distant rotating galaxy were available, then a shear signal should be detectable unambiguously without stacking or averaging images. The results of a maximum likelihood fit to the P.A. and  $i$ , taking into account both simulated position and velocity data are shown in Figure 3, for both zero shear and a typical shear value of 4%. An accurate self-consistent fit is obtained for zero shear, whose quality is significantly improved by including the velocity data, especially for low-inclination disks ( $i \simeq 0$ ). With shear, there is a clear offset between the best-fit values of the P.A. and  $i$  determined from the velocity and position data separately, the detection of which could be used to diagnose that significant shear is present in real data. The probability of the joint velocity-position fit is also reduced by a factor of about 2. For an almost edge-on disk ( $i \simeq \pi/2$ ), the extra information provided by velocity measurements is less significant, both for determining P.A. and for detecting a shear offset in the best-fit parameters. Projected circular rotating galaxies are good targets for measuring shear directly. Note that without measuring the velocity field, it is impossible to be sure that a galaxy is rotating and therefore accurately elliptical rather than just having a moderate intrinsic aspect ratio.

Figure 4 shows the results of fits to a common shear field  $\vec{\gamma}$  for simulated position and velocity data representing two disks with P.A.’s 45° apart. The P.A.’s are fixed, and assumed to be determined accurately from the velocity data. The maximum probability of the fit is shown for each value of  $\vec{\gamma}$  by solid lines, each of which is associated with a specific value of  $i$  for the best fit that is shown by dashed lines for the galaxy with P.A. =  $-0.285$  rad. There is a very significant degeneracy between the fitted values of  $\vec{\gamma}$  and  $i$ . The direction of this degenerate strip in the  $\vec{\gamma}$  plane is fixed by the P.A., and rotates by  $2\Delta\text{P.A.}$  if P.A. changes by  $\Delta\text{P.A.}$  Hence, observations of two galaxies that sample the same shear, with P.A.’s that differ by about 45° or 135°, can be used to determine the shear accurately and unambiguously, as shown by the overlapping solid contours in Figure 4. The target galaxies should be at comparable redshifts, to ensure that they sample the same foreground structure and the nearer galaxy does not significantly lens the farther one.

If more than two galaxies are observed, then the accuracy of the correspondence between the various tracks can be used as a test of the reliability of the method. Note that  $\vec{\gamma}$  measurements from the rotation curves of several galaxies do not rely on a correlation technique. Hence spin or alignment correlations between pairs of galaxies (Crittenden et al. 2001; Lee & Pen 2001) should not affect their accuracy, provided that the galaxy velocity fields are

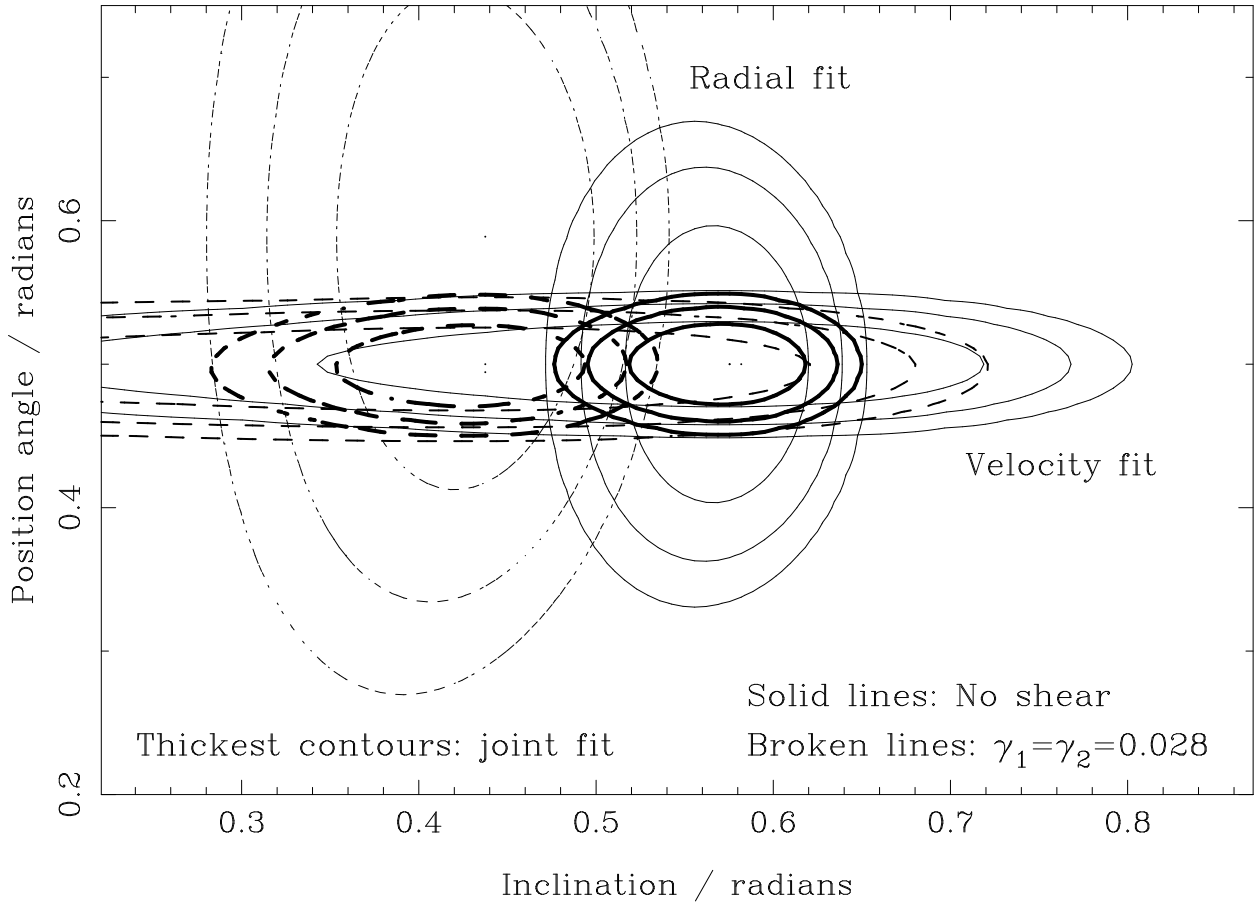


Fig. 3.— Likelihood ( $P$ ) contours obtaining by fitting the P.A. and  $i$  to simulated data from a rotating ring with P.A. = 0.5 and  $i$  = 0.57 rad, based on 100 data points with 5% accuracy for both position and velocity. The contours are all spaced by factors of 10 away from the peak value, and so the second contour corresponds approximately to a  $3\sigma$  error. With non-zero shear the quality of the joint radius-velocity fit to the P.A. and  $i$  is reduced from  $P \simeq 2.4 \times 10^{-5}$  to  $1.2 \times 10^{-5}$ . The velocity data always fixes the P.A. accurately.

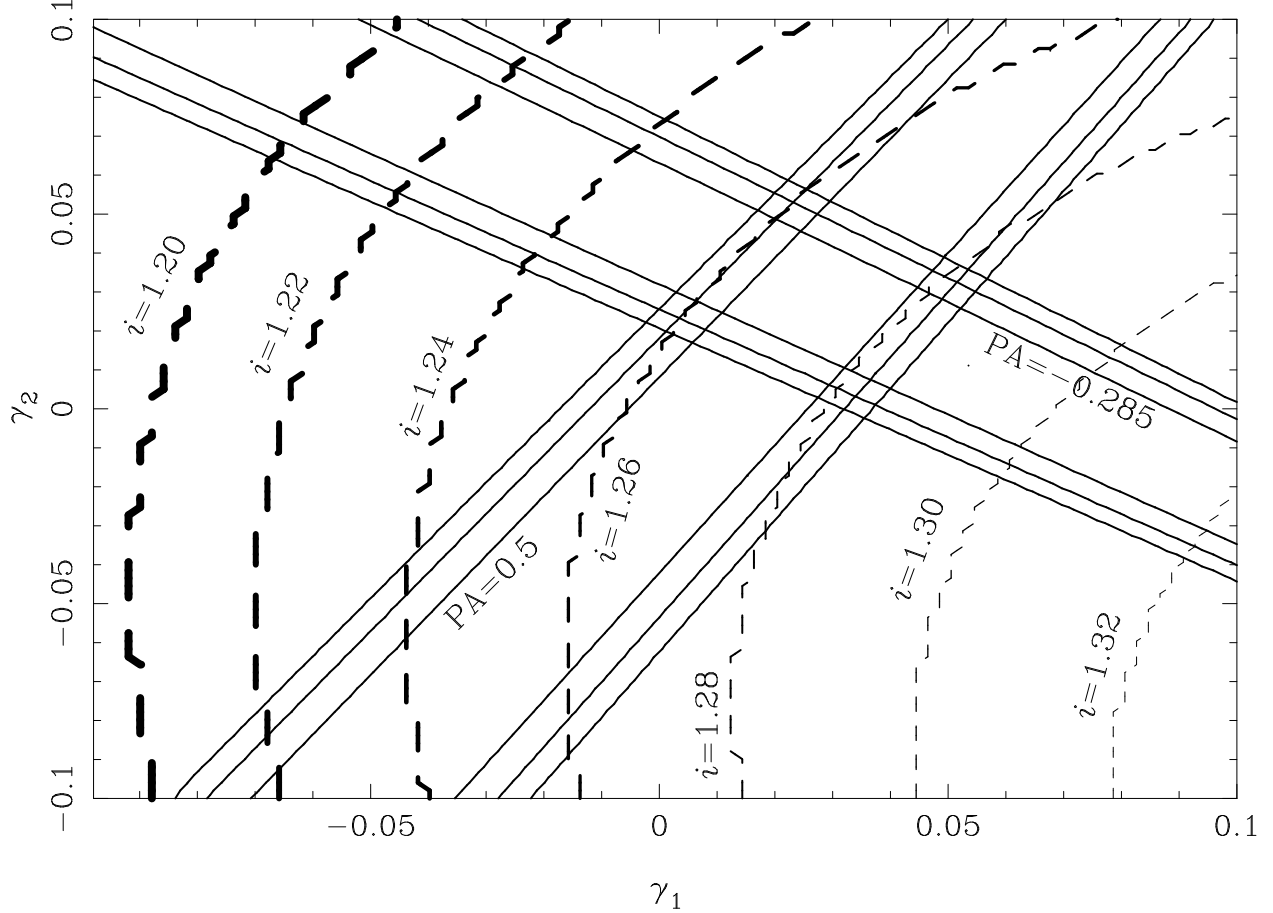


Fig. 4.— Results of fitting a common shear field using simulated data for two ring galaxies at inclination  $i = 1.27 \text{ rad}$  ( $72^\circ$ ), with P.A. = 0.5 and  $-0.285 \text{ rad}$  ( $\pi/4 \text{ rad}$  apart). The uncertainties in Fig. 3 are assumed. The solid lines show equal probabilities in the  $\vec{\gamma}$  plane, and are spaced by factors of 10 away from the best-fitting values ( $P = 7 \times 10^{-5}$ ). The values of  $i$  for which the joint probability of a fit to  $i$  and  $\vec{\gamma}$  is maximized are shown by the dashed lines for the P.A. =  $-0.285$  galaxy, demonstrating a powerful degeneracy between  $i$  and  $\vec{\gamma}$ . Prior information about the maximum value of  $|\vec{\gamma}|$  could be used to limit the extent of the probability contours in the degenerate direction. An unambiguous measurement of the input shear  $\vec{\gamma} = (0.028, 0.028)$  is obtained where the solid lines cross. The P.A. is determined accurately by the velocity data (see Fig. 3) and leads to very little degeneracy with  $\vec{\gamma}$ ; therefore, it is set to its fixed input value in the fitting process.

not distorted strongly by tidal interactions. Rather than determining a single average value of  $\vec{\gamma}$  over each  $10 \text{ arcmin}^2$  area of sky, or a correlation spectrum of  $\vec{\gamma}$  on scales of  $0'.5\text{--}10'$ , it should be possible to determine a value of  $\vec{\gamma}$  in a tube on the order of a few arcseconds wide along the line of sight to a specified point on the sky.

Such a measurement would provide a direct test of systematic effects in shape-based statistical shear measurements by comparing their results at specific positions. The shear from individual mass concentrations, including subcritical groups of galaxies, could be mapped in detail without stacking groups (Hoekstra et al. 2001) by measuring the shear along closely spaced lines of sight around the target. It may also be possible to probe for significant structure in the shear field on arcsecond angular scales, as expected if dark matter halos contain a large amount of substructure, by measuring differences in the shear field determined for galaxies only a few arcseconds apart.<sup>4</sup>

### 3. Requirements for detection

In order to exploit this effect, it will be necessary to measure very accurate rotation curves of distant galaxies. The shear signal is significant only at moderate redshifts ( $z > 0.3$ ; Bartelmann & Schneider 2001), at which the total extents of galaxies are only a few arcseconds. Sub- $0.1''$  spatial resolution is thus necessary. Measurements of velocity with 5%  $1-\sigma$  accuracy should be achievable based on low-redshift CO and HI observations of rotation curves traced by clouds with  $10 \text{ km s}^{-1}$  internal velocity dispersions and scatter from cloud to cloud. The errors expected from 100 simulated position-velocity data points of this accuracy are shown in Figure 3. Even in the most disturbed extra-nuclear molecular cloud regions, the maximum velocity dispersion is about  $20 \text{ km s}^{-1}$  (Bally et al. 1999). It is essential that the velocity field faithfully traces rotation, and is not due to outflowing gas moving at up to several  $100 \text{ km s}^{-1}$ , as is possible for optical nebular emission lines. The required sensitivity and resolution could probably be achieved either by using AO IFU spectroscopy of near-IR absorption or recombination lines or by measuring high-/low-excitation CO lines using ALMA/SKA or HI emission using SKA. We will consider the prospects for ALMA and SKA.

---

<sup>4</sup>Combining the measured CO rotation curve of highly inclined disks, which are often expected to strongly lens background galaxies (Blain, Möller & Maller 1999), with the positions of serendipitous multiple background images is unlikely to provide more accurate constraints on cosmological parameters than observing multiple images in rich clusters (Golse, Kneib, & Soucail 2002). Because both lensing and rotation-curve measurements are sensitive to the ratio of enclosed mass to radius, it is not possible to measure a ‘standard ruler’ across the galaxy to determine  $H_0$ .

The ALMA bands at 230 and 345 GHz can be used to detect CO lines excited in star-forming regions of ordinary disk galaxies at  $z \sim 0.5 - 1$ . CO is likely to be distributed within the inner several kiloparsecs of the disk, probably more centrally concentrated than the stellar light; however, there is a possibility that the CO emission may be concentrated very close to the nucleus, in which case resolved ALMA observations would be impossible, and centimeter-wave SKA observations of CO(1-0) or HI would be required. At 230 GHz, CO(3-2) from  $z \simeq 0.5$  and CO(4-3) from  $z \simeq 1$  can be detected. At 345 GHz, CO(5-4) can be detected from  $z \simeq 0.65$ . The expected luminosity can be calculated by scaling the high-resolution images of CO(1-0) from the low-redshift Berkeley–Illinois–Maryland Association Survey Of Nearby Galaxies (BIMA SONG; Regan et al. 2001) to higher redshifts and excitations or by scaling down the flux density of CO(3-2) detected in high-redshift ultraluminous galaxies (Frayer et al. 1999). The scaled-down high-redshift result implies a total integrated CO(3-2) line flux of  $0.5 \text{ Jy km s}^{-1}$  from  $z = 0.5$  for a Milky Way-like galaxy with a luminosity of about  $6 \times 10^{10} L_\odot$ . Scaling from CO(1-0) for NGC 4414 from BIMA SONG, assuming the Large Velocity Gradient model presented in Blain et al. (2000), line fluxes of 0.43, 0.49 and  $0.16 \text{ Jy km s}^{-1}$  are expected in CO(3-2) from  $z = 0.5$  at 230 GHz, CO(5-4) from  $z = 0.65$  at 345 GHz, and CO(4-3) from  $z = 1$  at 230 GHz, respectively. ALMA has a  $1\sigma$  sensitivity of 6.1 and  $11 \text{ mJy km s}^{-1}$  in the 230 and 345 GHz bands, respectively, for a 1 minute observation:  $70\sigma$ ,  $44\sigma$  and  $27\sigma$  detections are thus expected integrated over the whole disk of the galaxy in 1 minute for these three lines, respectively. For the most promising case, CO(3-2) from  $z = 0.5$ , this means that 100 independent spectra on the galaxy could be measured at  $10\sigma$  significance in about  $(100)^2/7^2$  minutes or 3.2 hr. At 230 GHz, ALMA has a maximum resolution of about 30 mas (on a 10 km baseline), and therefore has sufficient spatial and spectral resolution to measure  $\vec{\gamma}$ . Note that the time required to make a coarse measurement of the total luminosity and extent of CO emission using ALMA is very much less than that required to produce a fully resolved image for shear measurements. Hence, only galaxies that seem to be regular rotating disks in short snapshot observations need be subjected to 1–10 hr integrations to measure accurate rotation curves. The morphology of the dust emission from the target is determined simultaneously, for comparison with that of radio emission and near-IR/optical starlight.

The SKA detection limit for HI emission from  $z \simeq 1$  is several  $10^8 M_\odot$  in many tens of hours of integration. Hence, it should be possible to detect several tens of  $0''.1$  resolution elements across a high-redshift galaxy similar to the  $5 \times 10^9 M_\odot$  NGC 4414 in a reasonable time at 1 GHz, for baselines longer than about 600 km. SKA has a much larger field of view than ALMA and will image a very large number of galaxies simultaneously. As discussed in its web-based science case (see footnote 1) SKA could carry out conventional ‘statistical’ cosmic shear studies using just the shapes of galaxies.

In order to estimate the signal-to-noise ratio for the velocity measurements, a reasonable figure of merit is the product of the resolved area of the galaxy on the sky (which determines the number of independent velocity measurements) and the size of the change in the projected line-of-sight velocity across the disk. These functions depend on  $\cos i$  and  $\sin i$  respectively. Only in the most edge-on disks would CO emission be obscured by and blended with foreground clouds in the target galaxy, and therefore the total integrated flux in a CO line is not expected to depend on  $i$ . The figure of merit thus depends on  $\sin 2i$  and is maximized at  $i \simeq 45$  deg: edge-on galaxies yield too few independent data points, while the velocity gradient in face-on galaxies is too small to be sure that the motion is rotational.

The shear signal is expect to increase as  $z^{\simeq 0.6}$  at source redshifts  $z \simeq 0.5\text{--}1$  (Bartelmann & Schneider 2001). Note that the integrated flux of a line decreases as  $D_L^{-2}$ , and the number of resolved spectra decreases as  $D_A^{-2}$ , where  $D_L$  and  $D_A$  are the luminosity and angular diameter distances, respectively.  $D_A = D_L(1+z)^{-2}$ , leading to  $(1+z)^{-4}$  surface brightness dimming, and therefore it is easier to detect and resolve lines from galaxies at lower redshifts. A conservative figure of merit for the redshift dependence of the detectability of lines for measuring  $\vec{\gamma}$  would be  $D_L^{-2}$ , which decreases as  $z^{\simeq -2.4}$  from  $z \simeq 0.5\text{--}1$ , much more steeply than  $\vec{\gamma}(z)$  increases. This is before the likely systematic decrease in galaxy disk size/mass with increasing redshift is taken into account. Hence, in order to detect shear it is sensible to observe relatively low redshift galaxies: this favors 230 GHz ALMA observations of CO(3-2) from  $z \simeq 0.5$ .

#### 4. Caveats

In order to detect the velocity structure of weakly lensed galaxies and determine  $\vec{\gamma}$ , observations with very high spatial and spectral resolution are required. The measurements need to be accurate to within about 5%, and so low-level systematic effects could potentially confuse and affect the results. We have illustrated the effect for a ring geometry. Spatially resolved spectroscopy of any disk built from a series of circular rings should allow this signal to be extracted. Even a galaxy with a series of irregularly distributed knots within a disk or spiral structure without radial inflow should allow an accurate rotation curve to be derived. If appreciable inflow does occur, then the galaxy would quickly be recognized as a poor target for a deep rotation-curve measurement. Low-redshift galaxies observed in HI can be well fitted by circular rotation; however, the P.A. can vary with radius (e.g., Mulder & van Driel 1993). This type of effect could prevent the detection of weak shear ring by ring within the galaxy.

To measure shear, the detected velocities must be assumed to be associated with regular

circular orbits. If the galaxy has a bar, warp, or  $m_1$  asymmetry, then this model may not be adequate, and low-level corrections to a simple circular model may mimic weak lensing. Bars appear to be less common at high redshifts (Abraham et al. 1999); however, warps are likely to be more common since galaxy interactions are more common. At low redshifts, bars tend to affect the dynamics within 2–3 kpc of the centers of disks, while warps affect orbits outside 10 kpc. Their signatures should be easy to see after much shorter ALMA integrations than are required to detect accurate rotation curves. In order to assess the detailed feasibility of the proposed observations, very high resolution CO and HI rotation curves at radii  $\simeq 5$  kpc at low and moderate redshifts will be required to check for systematic effects.

## 5. Conclusions

The use of measured high-resolution rotation curves of distant disk galaxies to determine cosmic shear has been described. The effects of lensing on the velocity and position of gas clouds in the galaxy are different, and so adding velocity information can provide a much more accurate shear measurement than shape alone. By observing two or more galaxies at relative P.A.’s of about  $45^\circ$ , a direct measurement of the shear can be made, without requiring correlations or averages of large numbers of faint galaxy images. Such observations are not possible at present, but will become so with AO IFU spectrographs, and future radio and millimeter-wave interferometers. Velocity measurements are essential in order to be sure that the observed galaxy is rotating (and has an exact intrinsic elliptical morphology) and to allow searches for systematic deviations from uniform rotation.

I thank Eric Agol, Richard Ellis, Jean-Paul Kneib, Ole Möller, Priya Natarajan and Kartik Sheth for helpful conversations.

## REFERENCES

- Abraham, R. G., Merrifield, M. R., Ellis, R. S., Tanvir, N. R., & Brinchmann, J. 1999, MNRAS, 308, 569
- Bacon, D. J., Refregier, A., & Ellis, R. S. 2000, MNRAS, 318, 625
- Bally, J., Reipurth, B., Lada, C. J., & Billawala, Y., 1999, AJ, 117, 410
- Bartelmann, M., & Schneider, P. 2001, Physics Reports, 340, 291
- Blain, A. W., Frayer, D. T., Bock, J. J., & Scoville, N. Z., 2000, MNRAS, 313, 559.

- Blain, A. W., Möller, O., & Maller, A. H. 1999, MNRAS, 303, 423
- Crittenden, R. G., Natarajan, P., Pen, U.-L., & Theuns, T., 2001, ApJ, 559, 552
- Fischer, P., et al. 2000, AJ, 120, 1198
- Frayer, D. T., et al. 1999, ApJ, 514, L13
- Golse, G., Kneib, J.-P., & Soucail, G., 2002, A&A, in press (astro-ph/0103500)
- Hoekstra, H., et al. 2001, ApJ, 548, L5
- Lee, J., & Pen, U.-L. 2001, ApJ, 555, L106
- McKay, T. A., et al. 2002, ApJ, submitted
- Maoli, R., van Waerbeke, L., Mellier, Y., Schneider, P., Jain, B., Bernardeau, F., Erben, T., & Fort, B. 2001, A&A, 368, 766
- Mulder, P. S., & van Driel, W., 1993, A&A, 272, 63
- Narasimha, D., & Chitre, S. M., 1993, A&A, 280, 57
- Pirzkal, N., et al. 2001, A&A, 375, 351
- Regan, M. W., Thornley, M. D., Helfer, T. T., Sheth, K., Wong, T., Vodel, S. N., Blitz, L., & Bock, D. C.-J. 2001, ApJ, 561, 218
- Schneider, P., Ehlers, J., & Falco, E. E., 1992, Gravitational Lenses. Springer: Berlin
- van Waerbeke, L., et al. 2001, A&A, 374, 757
- Wilson, G., Kaiser, N., & Luppino, G. A., 2001, ApJ, 556, 601
- Wittman, D. M., Tyson, J. A., Kirkman, D., Dell'Antonio, I., & Bernstein, G. 2000, Nature, 405, 143
- Wootten, A. ed 2001, Science with the Atacama Large Millimeter Array, PASP Conf. Ser. vol. 235